fluids

MDPI

Article

Effects of Expelled Air during Filling Operations with Blocking Columns in Water Pipelines of Undulating Profiles

Vicente S. Fuertes-Miquel [1,*], Oscar E. Coronado-Hernández [2] and Alfonso Arrieta-Pastrana [2]

[1] Departamento de Ingeniería Hidráulica y Medio Ambiente, Universitat Politècnica de València, 46022 Valencia, Spain
[2] Instituto de Hidráulica y Saneamiento Ambiental, Universidad de Cartagena, Cartagena 130001, Colombia; ocoronadoh@unicartagena.edu.co (O.E.C.-H.); aarrietap2@unicartagena.edu.co (A.A.-P.)
* Correspondence: vfuertes@upv.es

Abstract: Entrapped air pockets can cause failure in water distribution systems if air valves have not been appropriately designed for expelling air during filling manoeuvres performed by water utilities. One-dimensional mathematical models recently developed for studying this phenomenon do not consider the effect of blocking columns inside water pipelines. This research presents the development of a mathematical model for analysing the filling process in a pipeline with an undulating profile with various air valves, including blocking columns during starting-up water installations. The results show how different air pocket pressure peaks can be produced over transient events, which need to be analysed to ensure a successful procedure that guarantees pipeline safety during the pressure surge occurrence. In this study, an experimental set-up is analysed to observe the behaviour of two blocking columns during filling by comparing the air pocket pressure pulses.

Keywords: entrapped air pocket; blocking column; filling operation; water distribution system

Citation: Fuertes-Miquel, V.S.; Coronado-Hernández, O.E.; Arrieta-Pastrana, A. Effects of Expelled Air during Filling Operations with Blocking Columns in Water Pipelines of Undulating Profiles. *Fluids* **2024**, *9*, 212. https://doi.org/10.3390/fluids9090212

Academic Editors: Kamil Urbanowicz and Kambiz Vafai

Received: 13 August 2024
Revised: 7 September 2024
Accepted: 10 September 2024
Published: 11 September 2024

1. Introduction

Transient events caused by air pockets inside pipelines have gained attention in the last decades since pressure surges can originate catastrophic scenarios that can produce the failure of hydraulic installations [1]. Most analysed scenarios assume the worst possible conditions, so the resulting air pocket pressure peaks represent the maximum values in water pipelines [2,3], which must be considered when selecting the pipe resistance class [4]. This makes studying this problem of practical interest for water utilities [5]. To avoid issues caused by entrapped air pockets, air valves are commonly installed at various points in the system [6,7]. These valves allow air to be expelled, reducing pressure surges in installations [8]. It is crucial to note that air valves do not always provide the expected reliability and can sometimes cause severe problems when they are undersized or when filling operations are not performed according to recommendations proposed by the American Water Works Association (AWWA) [9].

Despite the advantages of using air valves [10], they also present several challenges [11]. For instance, sizing and selecting air valves must be done carefully. Estimating the amount of expelled air is also challenging [12,13]. Oversizing, especially during air expulsion, can cause high overpressures, making it dangerous to select a valve that is either too small or too large [4].

Another significant issue is the proper static and dynamic modelling of these valves. While some manufacturers provide characteristic curves in their catalogues, these data are often unreliable. Various laboratories and universities, including the Polytechnic University of Valencia, have conducted static tests on different valves, and the results generally show significant discrepancies from the manufacturers' data [14]. This can lead to critical problems due to incorrect selection based on unsuitable characteristic curves. The situation regarding dynamic characterisation is even worse since there is a lack of available

information. Manufacturers overlook this aspect, and there is still much to be done from a research perspective.

Besides the difficulties in sizing air valves and the unreliability of manufacturers' characteristic curves, other issues include the "dynamic closure" of these devices (an air valve closing prematurely due to a lifting effect on the float, leaving a dangerous air pocket inside water installations), the poor correlation between the nominal diameter of an air valve (usually matching the connection diameter) and its expulsion capacity, and inadequate or non-existent maintenance, which can lead to malfunction when an air valve is needed [4]. Therefore, while air valves in hydraulic installations are highly recommended, they do not guarantee total safety. For the reasons stated above, these devices can cause more issues related to pressure surges than those they are intended to solve.

During the last decades, different mathematical models have been proposed. Martin (1976) [15] proposed the first system for analysing two-phase flows in confined pipeline systems, establishing a differential equations system composed of the continuity and momentum formulations and the thermodynamic behaviour of the air phase. Liou & Hunt (1996) [16] developed a rigid column model, applicable when high flow velocities and small pipe diameters are present. Izquierdo et al. (1999) [17] investigated scenarios involving irregular pipe profiles with entrapped air using the rigid column model. This model considers a perpendicular air-water interface (piston flow) representing rapid transients where some pipe sections are filled with air. In contrast, others are entirely occupied by water.

Wylie & Streeter (1993) [18] were the first to develop an elastic model that incorporates the elasticity of the fluid, focusing solely on single-phase flows. Zhou, Liu, and Karney (2013) [19] extended this elastic model to analyse filling processes by combining the continuity and momentum equations for the water phase with the polytropic equation governing the behaviour of the air phase. This model was developed for both simple and irregular pipe cases, accounting for entrapped air pockets within the system. More recently, Zhou et al. (2020) [12] studied, using a simple pipe, the effects occurring during rapid filling phenomena in an experimental setup measuring 8.862 m in length and 400 mm in internal diameter, with a 10-mm orifice added at the end to expel airflow.

The effects of blocking columns in confined hydraulic installations represent another critical issue that requires careful consideration. This is because the elasticity of air is significantly higher than that of water [20], leading to scenarios where water can easily compress air columns, potentially causing pressure surges in hydraulic systems. Although the effects of blocking columns have been explored regarding various entrapped air pockets using both elastic and rigid models [17,19], the literature reveals a gap in addressing these issues in systems with undulating pipe profiles, particularly when air valves or orifices sizes are installed during filling operations.

This research presents a mathematical model for studying transient events with entrapped air pockets, including air valves. This study provides a valid model for analysing transients generated by n entrapped air pockets in pipelines with irregular profiles and V installed air valves [21,22]. The proposed model's generalised equations, including the air valve's behaviour, are presented. The main advantage of the proposed model over previous ones is that it is suitable for considering the effects of blocking columns and air valves. Furthermore, this system of equations is particularised for a specific case: an installation with two entrapped air pockets and an air valve installed at the highest point of a water installation with an irregular profile. The problem involves the presence of a second air pocket [23]. A polytropic evolution was considered to characterise the behaviour of air pockets during transient events. A specific case is analysed using the obtained system of equations and its corresponding numerical resolution. The selected case study corresponds to a water installation located at the hydraulic laboratory at the Technical University of Valencia, Spain. Transient events are analysed considering two scenarios: first without air valves and then considering an air valve installed at the highest point in the pipeline.

The results for both situations are compared, observing the effect of air valves on the transient events. When the air pocket's location coincides with the air valve's position, the device allows free air expulsion, significantly smoothing the air compression process (reducing pressure peaks). However, when the water arrives and the air valve closes, the air pocket is again confined between two water columns with no escape to the atmosphere, leading to a new transient evolution similar to those studied without valves, generating the corresponding pressure peaks based on the conditions at the time of valve closure. Finally, this research analyses the same installation with different valve sizes. This allows for studying the effect of air valves' sizes and characteristics (mainly the expulsion coefficient and outlet size) on various transient events.

2. Mathematical Model

This section shows the mathematical model's development considering the air valves' behaviour. In this sense, a pipeline with an irregular profile and an air valve at the highest point in the installation is considered. At this point, an air pocket is initially trapped between two water columns (Figure 1).

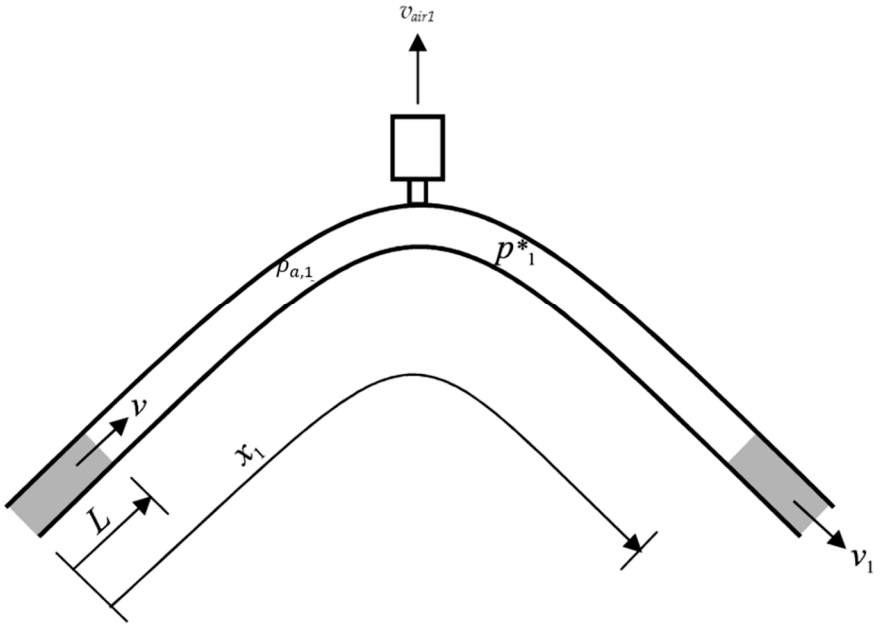

Figure 1. Installation of an air release valve.

The governing equations are presented below, considering the following assumptions: (i) water movement is simulated using the rigid water column model; (ii) a polytropic law is suitable for following the behaviour of entrapped air pockets; (iii) the air-water interface is considered perpendicular with the main direction of the pipe, which is applicable for pipelines with small internal diameters; (iv) a friction factor using steady flow conditions is considered; and (v) an isentropic flow is considered for the expelled air.

For a filling column, there are two equations:

1. Equation of the rigid model characterising the motion of the filling column driven by an energy source (p_0^* = upstream pressure in the pipeline; p_1^* = air pocket pressure)

$$\frac{dv}{dt} = \frac{p_0^* - p_1^*}{\rho L} - g\frac{\Delta z}{L} - \frac{fv|v|}{2D}, \tag{1}$$

where v = water velocity, f = friction factor, D = internal pipe diameter, Δz = difference elevation between two points of a water column, $\Delta z/L$ = gravity term, ρ = water density, L = length a water column, and g = gravitational acceleration.

2. Position of the filling column

$$L = L_0 + \int_0^t v dt, \tag{2}$$

where the subscript 0 refers to an initial condition.

For an air pocket, there are three equations:

3. Evolution of the air pocket (assuming a polytropic evolution)

$$\frac{dp_1^*}{dt} = k\frac{p_1^*}{\forall_1}\frac{d\forall_1}{dt} + \frac{p_1^*}{\forall_1}\frac{k}{\rho_{a,1}}\frac{dm_{\mathrm{a},1}}{\mathrm{dt}}, \tag{3}$$

where $m_{\mathrm{a},1}$ = air mass, k = polytropic coefficient, and $\forall_1$ = air pocket volume. The subscript 1 refers to the condition of the air pocket. The polytropic coefficient varies from 1.0 (isothermal evolution) to 1.4 (adiabatic condition).

4. Continuity equation for an air pocket (considering that the air pocket density ($\rho_{\mathrm{a},1}$) and air density at the outlet section (ρ_{air1}) are equal)

$$\frac{dm_{\mathrm{a},1}}{dt} = -\rho_{\mathrm{a},1} v_{air1} A_{exp}, \tag{4}$$

where v_{air1} = air velocity and A_{exp} = cross-sectional area of an air valve.

Defining the air mass:

$$\frac{d(\rho_{\mathrm{a},1}\forall_1)}{dt} = -\rho_{\mathrm{a},1} v_{air1} A_{exp}, \tag{5}$$

Solving the derivate:

$$\frac{d\rho_{\mathrm{a},1}}{dt}\forall_1 + \rho_{\mathrm{a},1}\frac{d\forall_1}{dt} = -\rho_{\mathrm{a},1} v_{air1} A_{exp}, \tag{6}$$

Considering that:

$$\begin{cases} \forall_1 = (x_1 - L)A \\ \frac{d\forall_1}{dt} = (v_1 - v)A \end{cases} \tag{7}$$

where A = cross-sectional area of the pipe, x_1 = position of the water column, and v_1 = water velocity of a blocking column.

Organising terms:

$$\frac{d\rho_{\mathrm{a},1}}{dt}(x_1 - L)A + \rho_{\mathrm{a},1}(v_1 - v)A = -\rho_{\mathrm{a},1} v_{air1} A_{exp}, \tag{8}$$

Solving for the air density:

$$\frac{d\rho_{\mathrm{a},1}}{dt} = \frac{-\rho_{\mathrm{a},1} v_{air1} A_{exp} - \rho_{\mathrm{a},1}(v_1 - v)A}{(x_1 - L)A}, \tag{9}$$

5. Equation modelling the behaviour of the air release valve

During the pipeline filling process, it is typical that air valves operate in the subsonic flow range (p_1^* < 19.55 m = 1.918 bar). The behaviour of expelled air in the subsonic region follows a simple expression that relates the expelled airflow Q_{air1} under normal conditions (1 atm and 15 °C, that is, a density $\rho_{a,N} = 1.205\ \mathrm{kg/m^3}$) with the pressure inside a pipeline p_1^*. The corresponding equation is given by:

$$Q_{air1} = c_{exp}\sqrt{(p_1^* - p_{atm}^*)p_1^*}, \tag{10}$$

where c_{exp} = expelled coefficient of an air valve and p_{atm}^* = atmospheric pressure.

From this, the air expulsion velocity v_{air1} can be determined:

$$\rho_{a,N} Q_{air1} = \rho_{a,1} v_{air1} A_{exp}, \tag{11}$$

where $\rho_{a,N}$ = air density at atmospheric conditions (1.205 kg/m^3).

Equation (11) can be expressed as:

$$v_{air1} = \frac{1.205}{\rho_{a,1}} \frac{c_{exp}}{A_{exp}} \sqrt{(p_1^* - p_{atm}^*) p_1^*}, \tag{12}$$

If a filling operation were a perfectly controlled process, it would proceed slowly, and air valves would operate in the subsonic range. However, when a pipeline filling occurs more abruptly, the pressure in hydraulic installations may exceed the subsonic flow limit ($p_1^* \geq 19.55\,\text{m} = 1.918\,\text{bar}$); in this case, the expelled air is found in the sonic flow regime. The behaviour of an air valve in the sonic region fits well with a straight line, meaning the relationship between the expelled airflow under normal conditions Q_{air1} and the pressure inside in a pipeline p_1^* is linear. To extend the previous equation and thus have a valid expression for the sonic flow region, this line has the same slope as the one at the limit point ($p_1^* = 19.55\,\text{m}$) when the flow is subsonic. Therefore, the line should pass through the point $Q_{air1} = 13.426 c_{exp}$ and $p_1^* = 19.55$ m. The slope of this line is:

$$\text{slope} = \left.\frac{dQ_{air1}}{dp_1^*}\right|_{p_1^*=19.55} = c_{exp} \frac{2p_1^* - p_{atm}^*}{2\sqrt{(p_1^* - p_{atm}^*) p_1^*}} = 1.071, \tag{13}$$

Thus, the expression that simulates the behaviour of the expelled air when an air valve is operating in the sonic region (when $p_1^* \geq 19.55\,\text{m}$) is:

$$Q_{air1} = -7.521 c_{exp} + 1.071 c_{exp} p_1^*, \tag{14}$$

Expressing this line in terms of the air velocity v_{air1} is as follows:

$$v_{air1} = \frac{1.205}{\rho_{a,1}} \frac{c_{exp}}{A_{exp}} (-7.521 + 1.071 \rho_1), \tag{15}$$

For a blocking column, there are two equations:

6. Equation of the rigid model characterizing the movement of a blocking column (p_1* is the pressure of the air pocket and p_{atm}^* is atmospheric pressure)

$$\frac{dv_1}{dt} = \frac{p_1^* - p_{atm}^*}{\rho L_{b,1}} - g \frac{\Delta z_{b,1}}{L_{b,1}} - \frac{f v_1 |v_1|}{2D}, \tag{16}$$

where $L_{b,1}$ = length of the blocking column and $\frac{\Delta z_{b,1}}{L_{b,1}}$ = gravity term of the blocking column.

7. Position of a blocking column

$$x_1 = x_{1,0} + \int_0^1 v_1 dt \text{ or } \frac{dx_1}{dt} = v_1, \tag{17}$$

Therefore, a system composed of 7 equations needs to be solved. The 7 unknown variables for the analysed problem are:

Two unknowns for the filling column:

- Water velocity v and position L

Three unknowns for the air pocket:

- Expulsion velocity v_{air1}, pressure p_1^*, and density $\rho_{a,1}$

Two unknowns for the blocking column:

- Velocity v_1 and position x_1

This system of equations remains valid until the filling column reaches the position of an air valve. At that moment, the water pressure will cause the float to rise, closing the valve and nullifying the air expulsion velocity ($v_{air1} = 0$).

In this new situation, the equation modelling the air valve's behaviour (Equations (12) and (15)), depending on whether it operates in the subsonic or sonic zone, respectively, is removed from the system. Then, a system of 6 equations with 6 unknowns (v, Lv_1, x_1, p_1^*, $\rho_{a,1}$) needs to be solved. The continuity equation for the air pocket (Equation (9)) can be neglected because the computation of the air density $\rho_{a,1}$ is no longer necessary; thus, Equation (3) becomes:

$$p_1^*(x_1 - L)^k = p_{1,0}^*(x_{1,0} - L_0)^k = \text{constant} \tag{18}$$

Equation (18) maintains the assumption of a polytropic evolution when an air valve closes and an air pocket is trapped. A water utility's standard procedure for cleaning and maintaining water pipelines involves starting them up. This process begins when the pipeline is at rest because the regulating valves are closed.

3. Description for Two Entrapped Air Pockets and an Air Valve

3.1. Governing Equations

The proposed model is presented for an installation with four pipe branches of constant slope ($m = 4$) and two entrapped air pockets ($n = 2$) where there is an air valve ($V = 1$) at the highest point of the profile (see Figure 2).

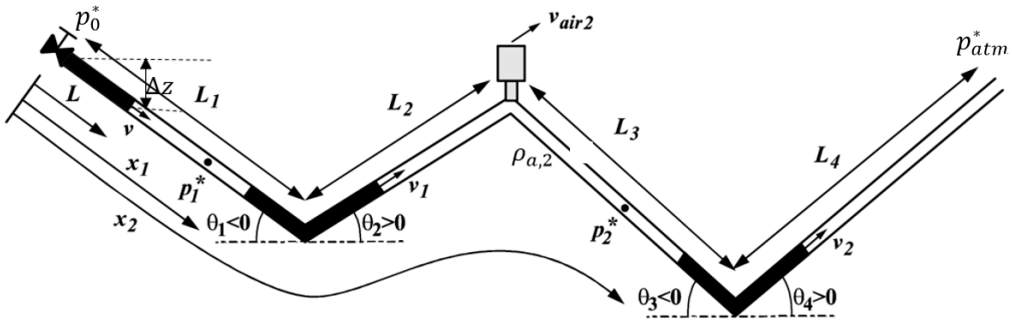

Figure 2. Installation with two entrapped air pockets and an air release valve (Phase A).

Ten equations must be used to model the pipeline filling for an installation with two entrapped air pockets and an air valve. The different phases of this process are presented below.

3.1.1. Phase A

The system starts at rest ($t = 0$), as depicted in Figure 2. The system of equations for modeling this problem are described as follows:

- For the filling column:

1. Equation of the rigid model to consider the movement of the filling column (p_0^* is the upstream pressure in the pipeline and p_1^* is the pressure of the first air pocket)

$$\frac{dv}{dt} = \frac{p_0^* - p_1^*}{\rho L} - g\frac{\Delta z}{L} - \frac{fv|v|}{2D}, \tag{19}$$

2. Position of the filling column

$$L = L_0 + \int_0^t v dt \quad \left(\frac{dL}{dt} = v\right), \tag{20}$$

- For the first air pocket, there is 1 equation:

3. Evolution of air pocket 1 (polytropic law)

$$p_1^*(x_1 - L)^k = p_{1,0}^*(x_{1,0} - L_0)^k = \text{constant}. \tag{21}$$

- For the first blocking column, there are 2 equations:

4. Equation of the rigid model that characterizes the movement of blocking column 1 (p_1^* is the pressure of the first air pocket and p_2^* is the pressure of the second air pocket)

$$\frac{dv_1}{dt} = \frac{p_1^* - p_2^*}{\rho L_{b,1}} - g\frac{\Delta z_{b,1}}{L_{b,1}} - \frac{f v_1 |v_1|}{2D}, \tag{22}$$

5. Position of blocking column 1

$$x_1 = x_{1,0} + \int_0^t v_1 dt \qquad \left(\frac{dx_1}{dt} = v_1\right), \tag{23}$$

For the last air pocket, there are 3 equations:

6. Evolution of air pocket 2 (assuming a polytropic evolution)

$$\frac{dp_2^*}{dt} = k\frac{p_2^*}{\forall_2}\frac{d\forall_2}{dt} + \frac{p_2^*}{\forall_2}\frac{k}{\rho_{a,2}}\frac{dm_{a,2}}{dt}, \tag{24}$$

7. Continuity equation for air pocket 2 (applying a similar procedure described in Section 2)

$$\frac{dm_{a,2}}{dt} = -\rho_{a,2} v_{air2} A_{exp}, \tag{25}$$

$$\frac{d(\rho_{a,2}\forall_2)}{dt} = -\rho_{a,2} v_{air2} A_{exp}, \tag{26}$$

$$\frac{d\rho_{a,2}}{dt}\forall_2 + \rho_{a,2}\frac{d\forall_2}{dt} = -\rho_{a,2} v_{air2} A_{exp}, \tag{27}$$

$$\forall_2 = (x_2 - x_1 - L_{b,1})A, \tag{28}$$

$$\frac{d\forall_2}{dt} = (v_2 - v_1)A, \tag{29}$$

$$\frac{d\rho_{a,2}}{dt}(x_2 - x_1 - L_{b,1})A + \rho_{a,2}(v_2 - v_1)A = -\rho_{a,2} v_{air2} A_{exp}, \tag{30}$$

$$\frac{d\rho_{a,2}}{dt} = \frac{-\rho_{a,2} v_{air2} A_{exp} - \rho_{a,2}(v_2 - v_1)A}{(x_2 - x_1 - L_{b,1})A}, \tag{31}$$

where subscript 2 refers to the second air pocket.

8. Equation for the air valve characterisation

Subsonic flow region ($p_2^* < 19.55\,\text{m} = 1.918\,\text{bar}$):

$$Q_{air2} = c_{exp}\sqrt{(p_2^* - p_{atm}^*)p_2^*}, \tag{32}$$

$$v_{air2} = \frac{1.205}{\rho_{a,2}}\frac{c_{exp}}{A_{exp}}\sqrt{(p_2^* - p_{atm}^*)p_2^*}, \tag{33}$$

Sonic flow region ($p_2^* \geq 19.55\,\text{m} = 1.918\,\text{bar}$):

$$Q_{air2} = -7.521 c_{exp} + 1.071 c_{exp} p_2^*, \tag{34}$$

$$v_{air2} = \frac{1.205}{\rho_{a,2}}\frac{c_{exp}}{A_{exp}}(-7.521 + 1.071 p_2^*), \tag{35}$$

For the last blocking column, there are 2 equations:

9. Equation of the rigid model characterizing the movement of blocking column 2 (p_2^* is the pressure of the second air pocket and p_{atm}^* is the downstream pressure of the pipeline)

$$\frac{dv_2}{dt} = \frac{p_2^* - p_{atm}^*}{\rho L_{b,2}} - g\frac{\Delta z_{b,2}}{L_{b,2}} - \frac{f v_2 |v_2|}{2D}, \tag{36}$$

10. Position of blocking column 2

$$x_2 = x_{2,0} + \int_0^t v_2 dt \quad \left(\frac{dx_2}{dt} = v_2\right), \tag{37}$$

where $L_{b,2}$ = length of the blocking column 2, $\frac{\Delta z_{b,2}}{L_{b,2}}$ = gravity term of the blocking column 2, and v_2 = water velocity of the blocking column 2.

This results in a system of 10 equations, the resolution of which, along with the initial conditions ($t = 0$) and the corresponding boundary conditions (p_0^* and p_{atm}^*), are needed to compute the 10 unknowns of the problem, which are:

- Two unknowns for the filling column: v, L
- One unknown variable for the air pocket 1: p_1^*
- Two unknowns for the blocking column 1: v_1, x_1
- Three unknowns for the air pocket 2: v_{air2}, p_2^*, $\rho_{a,2}$
- Two unknowns for the blocking column 2: v_2, x_2

3.1.2. Phase B

The previous system of equations is only valid while the air valve is expelling air, that is, until the first blocking column reaches the position of the valve ($x_1 + L_{b,1} = x_{v1}$). The air valve closes from this moment and the air expulsion velocity will become zero ($v_{air2} = 0$).

Since the air valve no longer functions in this phase (see Figure 3), the corresponding equation that models the air valve's behaviour can be neglected (Equations (33) and (35)), depending on whether the flow is subsonic or sonic.

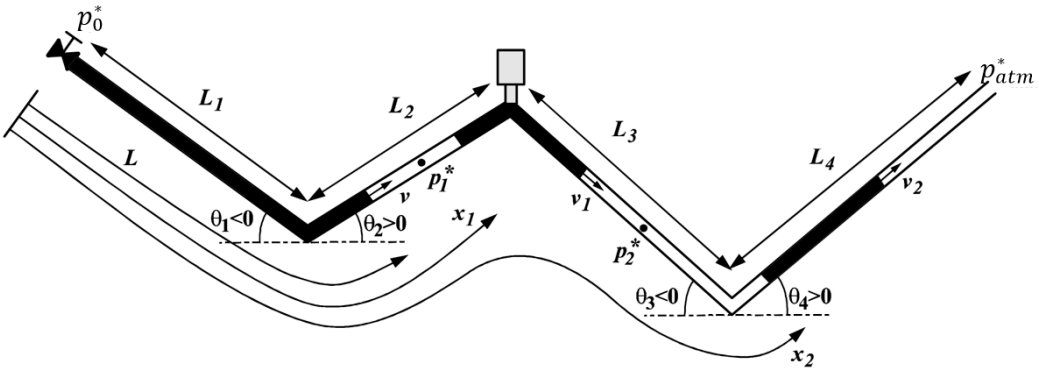

Figure 3. Phase B of the transient event for the two entrapped air pockets and an air valve.

Thus, for this phase of the transient, there is a system composed of 9 equations with 9 unknown variables (v, L, v_1, x_1, p_1^*, v_2, x_2, p_2^*, $\rho_{a,2}$). This system can be simplified by omitting the continuity equation for the second air pocket (Equation (31)), as it is no longer necessary to calculate the air density ρ_2 to solve the problem. Then, the system is reduced to 8 equations with 8 unknown variables (v, L, v_1, x_1, p_1^*, v_2, x_2, p_2^*). Equation (25) can be written as follows:

$$p_2^*(x_2 - x_1 - L_{b,1})^k = p_{2,0}^*(x_{2,0} - x_{1,0} - L)^k = \text{constant}, \tag{38}$$

3.1.3. Phase C

This new situation remains until the first air pocket reaches the position of the air valve ($x_1 = x_{v1}$). The air valve opens by expelling air, as shown in Figure 4.

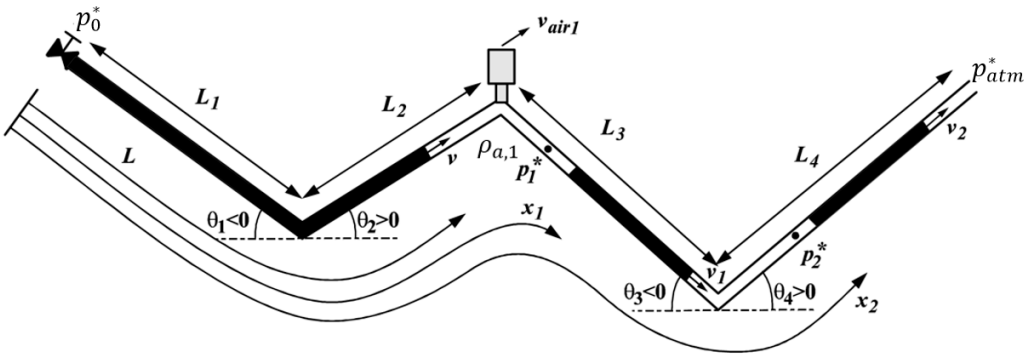

Figure 4. Phase C of the transient event for the two entrapped air pockets and an air valve.

As in the first phase, a system of 10 equations with ten unknowns is obtained:
For the filling column, there are 2 equations:
1. Equation of the rigid model characterizing the movement of the filling column

$$\frac{dv_2}{dt} = \frac{p_0^* - p_1^*}{\rho L} - g\frac{\Delta z}{L} - \frac{fv|v|}{2D}, \tag{39}$$

2. Position of the filling column

$$L = L_0 + \int_0^t v dt \;\; \frac{dL}{dt} = v, \tag{40}$$

For the first air pocket, there are 3 equations:
3. Evolution of air pocket 1 (considering a polytropic evolution)

$$\frac{dp_1^*}{dt} = k\frac{p_1^*}{\forall_1}\frac{d\forall_1}{dt} + \frac{p_1^*}{\forall_1}\frac{k}{\rho_{a,1}}\frac{dm_{a,1}}{dt}, \tag{41}$$

4. Continuity equation for air pocket 1

$$\frac{d\rho_{a,1}}{dt} = \frac{-\rho_{a,1}v_{air1}A_{exp} - \rho_{a,1}(v_1 - v)A}{(x_1 - L)A}, \tag{42}$$

5. Equation for modelling the behaviour of the air valve
Subsonic flow region ($p_1^* < 19.55\,\text{m} = 1.918\,\text{bar}$)

$$Q_{air1} = c_{exp}\sqrt{(p_1^* - p_{atm})p_1^*}, \tag{43}$$

$$v_{air1} = \frac{1.205}{\rho_{a,1}}\frac{c_{exp}}{A_{exp}}\sqrt{(p_1^* - p_{atm})p_1^*}, \tag{44}$$

Sonic flow region ($p_1^* \geq 19.55\,\text{m} = 1.918\,\text{bar}$)

$$Q_{air1} = -7.521c_{exp} + 1.071c_{exp}p_1^*, \tag{45}$$

$$v_{air1} = \frac{1.205}{\rho_{a,1}}\frac{c_{exp}}{A_{exp}}(-7.521 + 1.071p_1^*), \tag{46}$$

For the first blocking column, there are 2 equations:

6. Equation of the rigid model characterizing the movement of blocking column 1

$$\frac{dv_2}{dt} = \frac{p_1^* - p_2^*}{\rho L_{b,1}} - g\frac{\Delta z_{b,1}}{L_{b,1}} - \frac{f v_1 |v_1|}{2D}, \tag{47}$$

7. Position of blocking column 1

$$x_1 = x_{1,0} + \int_0^t v_1 dt \left(\frac{dx_1}{dt} = v_1\right), \tag{48}$$

8. Evolution of air pocket 1

$$p_2^*(x_2 - x_1 - L_{b,1})^k = p_{2,0}^*(x_{2,0} - x_{1,0} - L_{b,1})^k = \text{constant}, \tag{49}$$

For the last blocking column, there are 2 equations:
9. Equation of the rigid model characterizing the movement of blocking column 2

$$\frac{dv_2}{dt} = \frac{p_2^* - p_{atm}^*}{\rho L_{b,2}} - g\frac{\Delta z_{b,2}}{L_{b,2}} - \frac{f v_2 |v_2|}{2D}, \tag{50}$$

10. Position of blocking column 2

$$x_2 = x_{2,0} + \int_0^t v_2 dt \left(\frac{dx_2}{dt} = v_2\right), \tag{51}$$

The solution of this system composed of 10 equations, along with the initial conditions ($t = 0$) and boundary conditions (p_0^* y p_{atm}^*), must be solved to determine the 10 unknowns of the problem posed:

- Two unknowns for the filling column: v, L
- Three unknowns for air pocket 1: v_{aire1}, p_1^*, $\rho_{a,1}$
- Two unknowns for blockage column 1: v_1, x_1
- One unknown for air pocket 2: p_2^*
- Two unknowns for blockage column 2: v_2, x_2

3.1.4. Phase D

This system of equations is valid only until the filling column reaches the position of the air release valve ($L = x_{v1}$). The air valve closes again at that moment and the air expulsion velocity is null ($v_{aire1} = 0$).

Since the air valve is inactive during this transient phase (Figure 5), the equation is neglected.

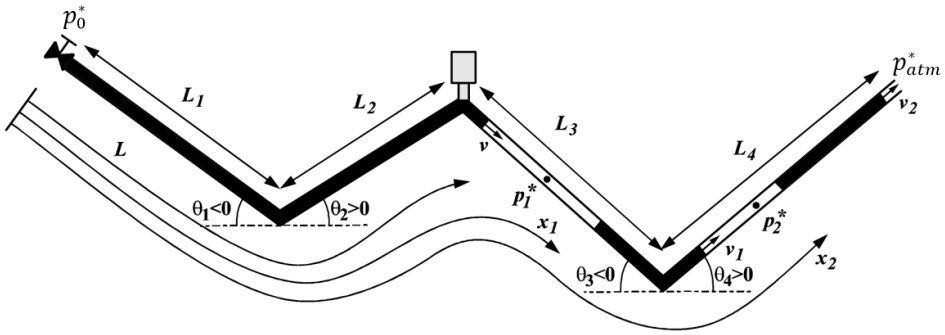

Figure 5. Phase D of the transient event for two entrapped air pockets and an air valve.

Therefore, the system that simulates the problem consists of a total of 9 equations with 9 unknown variables (v, L, v_1, x_1, p_1^*, $\rho_{a,1}$, v_2, x_2, p_2^*). Equation (4) can be omitted since

there is no need to calculate the air density $\rho_{a,1}$. Thus, the system is reduced to 8 equations with 8 unknown variables (v, L, v_1, x_1, p_1^*, v_2, x_2, p_2^*), where Equation (41) becomes:

$$p_1^*(x_1 - L)^k = p_{1,0}^*(x_{1,0} - L_0)^k = \text{constant}, \tag{52}$$

3.1.5. Phase E

The previous situation persists as long as there are two air pockets and two blocking columns. When the last water column completely leaves the water installation ($x_2 = L_{total}$), a new phase begins. There is only one blocking column and air pocket (Figure 6).

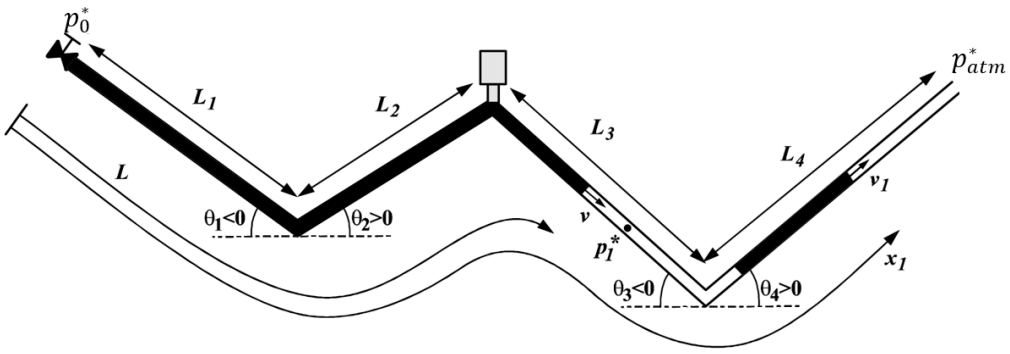

Figure 6. Phase E of the transient event for two entrapped air pockets and an air valve.

In this transient phase, all equations corresponding to the last blocking column and the last air pocket disappear. The downstream pressure of the blocking column becomes ($p_2^* = p_{atm}^*$) at the atmospheric conditions, resulting in the following system of equations:

$$\frac{dv}{dt} = \frac{p_0^* - p_1^*}{\rho L} - g\frac{\Delta z}{L} - \frac{fv|v|}{2D}, \tag{53}$$

$$L = L_0 + \int_0^t v dt \quad \left(\frac{dL}{dt} = v\right), \tag{54}$$

$$p_1^*(x_1 - L)^k = p_{1,0}^*(x_{1,0} - L_0)^k = \text{constant}, \tag{55}$$

$$\frac{dv_1}{dt} = \frac{p_1^* - p_{atm}^*}{\rho L_{b,1}} - g\frac{\Delta z_{b,1}}{L_{b,1}} - \frac{fv_1|v_1|}{2D}, \tag{56}$$

$$x_1 = x_{1,0} + \int_0^t v_1 dt \left(\frac{dx_1}{dt} = v_1\right), \tag{57}$$

The system of equations modelling the installation during this phase of the filling procedure, where there is only one entrapped air pocket, has been reduced to 5 equations with 5 unknown variables (v, L, v_1, x_1, p_1^*).

3.1.6. Phase F

The previous phase ends when the only remaining blocking column completely comes out the installation ($x_1 = L_{total}$). At this point, the existing air pocket disappears, leaving only the filling column, which partially occupies the installation (Figure 7).

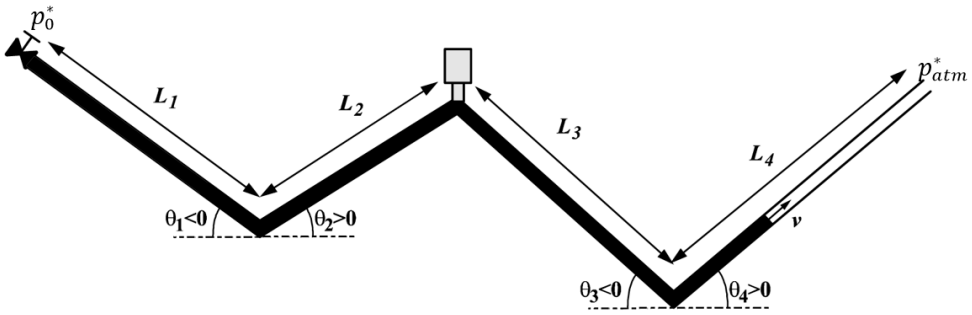

Figure 7. Phase F of the transient event for two entrapped air pockets and an air valve.

Under these conditions, the equations corresponding to the first blocking column and air pocket disappear. The filling column's downstream pressure becomes atmospheric ($p_1^* = p_{atm}^*$), reducing the system to two equations:

$$\frac{dv}{dt} = \frac{p_0^* - p_{atm}^*}{\rho L} - g\frac{\Delta z}{L} - \frac{fv|v|}{2D}, \tag{58}$$

$$L = L_0 + \int_0^t v dt \quad \left(\frac{dL}{dt} = v\right), \tag{59}$$

Transient modelling during the filling process can be carried out in this phase where there are no longer any air pockets, using a system of 2 equations with 2 unknown variables (v, L).

3.1.7. Phase G

Finally, when the filling column reaches the end of the hydraulic installation and begins to drain ($L = L_{total}$), the last phase of the transient event begins. The length of the filling column remains constant ($L = constant$) and the rigid model can be used to characterise the movement of the water column:

$$\frac{dv}{dt} = \frac{p_0^* - p_{atm}^*}{\rho L} - g\frac{\Delta z}{L} - \frac{fv|v|}{2D}, \tag{60}$$

This differential equation models the final stage of the transient until it reaches the steady state.

3.2. Numerical Resolution

The most general case involves the presence of entrapped air pockets and various installed air valves along hydraulic pipelines. This scenario requires solving a system of $2 + 3n + 2V$ equations that determine the behaviour of the filling column (length L and velocity v) and three unknowns associated with each filling column and entrapped air pockets (upstream boundary position x_i, trapped air pocket pressure p_i^*, and blocking column velocity v_i), as well as two unknown variables for each installed air valve (air expulsion velocity $v_{air,r}$ and density of the air pocket exiting through the device $\rho_{a,r}$).

There is a system of $2 + 3n + 2V$ differential equations that must be solved. It is a nonlinear initial value problem, yet it meets the necessary assumptions to ensure the existence of a mathematical solution.

The resolution can be obtained using an appropriate numerical method. An adaptive step method was selected. The primary reason is that the transient phases involve abrupt changes in variables (requiring very small integration steps), while other phases are much smoother (allowing for larger integration steps). Therefore, the adaptive fifth-order Runge-Kutta method is suitable for this problem.

It is essential to highlight that the filling process constitutes a transient phenomenon characterised by distinct phases governed by different equations. In summary, the numeri-

cal resolution of the phenomenon involves solving a sequence of initial value problems with a decreasing number of differential equations. The initial condition for each issue is the final state of the previous system, with variables no longer holding physical significance.

4. Analysis of Results and Discussion

4.1. Practical Application

The proposed model is applied to study the filling of a system with four pipe branches of constant slope ($m = 4$), two air pockets ($n = 2$), and one air valve ($V = 1$) installed at the highest point in the pipeline of irregular profile.

An experimental facility was configured at the Technical University of Valencia, Spain (see Figure 8). This installation is fed using a pump, which was tested in the experimental facility. The pump curve is $H_b(\mathrm{m}) = 38.68 - 19.76\ Q\ (\mathrm{l/s})^2$. It discharges into the atmosphere in a reservoir. The pipeline has a total length (L_{total}) of 8.62 m, a diameter (D) of 18.8 mm, and a friction factor (f) of 0.020. Once a steady-state regime is established, the flow rate is $Q_{\mathrm{steady}} = 0.954 \frac{l}{s}$ (with a velocity of $v_{\mathrm{steady}} = 3.437 \frac{m}{s}$). The steady state was reached at the end of the transient event, which was considered by numerical and experimental results.

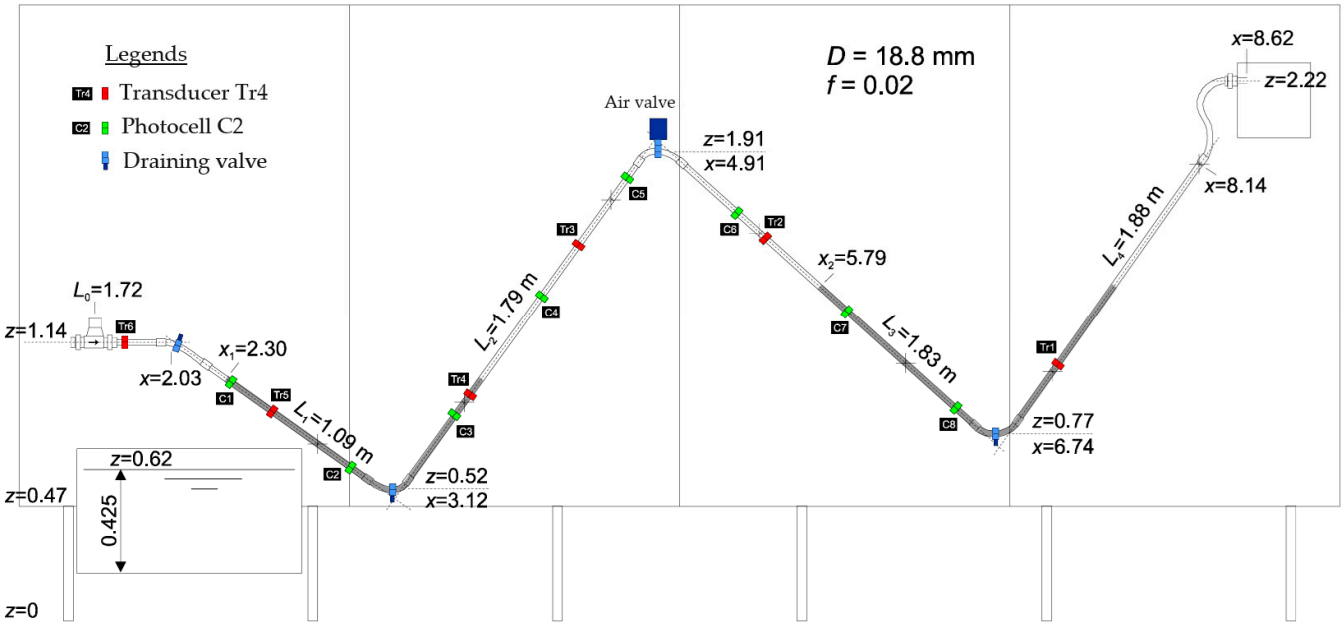

Figure 8. Experimental facility (installation with two entrapped air pockets and an air valve).

For the practical application, the initial positions of the blocking columns and, consequently, the initial sizes of the air pockets are:

- $x_{1,0} = 2.30\,\mathrm{m}$ ($L_{b,1} = 1.443\,\mathrm{m}$, $L_{air1,0} = 0.58\,\mathrm{m}$, $\forall_{1,0} = 0.161\,\mathrm{l}$)
- $x_{2,0} = 5.79\,\mathrm{m}$ ($L_{b,2} = 1.725\,\mathrm{m}$, $L_{air2,0} = 2.047\,\mathrm{m}$, $\forall_{2,0} = 0.5682\,\mathrm{l}$)

Once the pump is turned on, the discharge electro-valve is opened, thus beginning the pipeline's filling operation.

4.2. Installation without Air Valves

Solving the corresponding system of equations yields the results depicted graphically in Figure 9. This figure presents the pressure evolution of the two air pockets throughout the transient process. To measure the pressure pulses of the air pockets, transducers Tr3, Tr4, and Tr5 were used [20]. At the onset of the transient event, air pocket 1 is positioned at the location of Tr5, and the peak value predicted by the proposed model is 18.577 m at 0.19 s, which closely matches the experimental measurement of 17.484 m. A similar correspondence is observed with air pocket 2 and transducer Tr3. It is crucial to emphasise

that monitoring air pockets should consider the different transducers used. In this sense, the proposed model was used. Figure 9 shows, in purple colour, the difference between the computed (continuous line) and measured (discontinuous line) position of transducer Tr5, where the proposed model can follow the air pocket pulses during the transient event. The proposed model is suitable for predicting extreme pressure pulses for both air pockets. Similarly, Figure 10 shows the water velocity evolution of the three water columns.

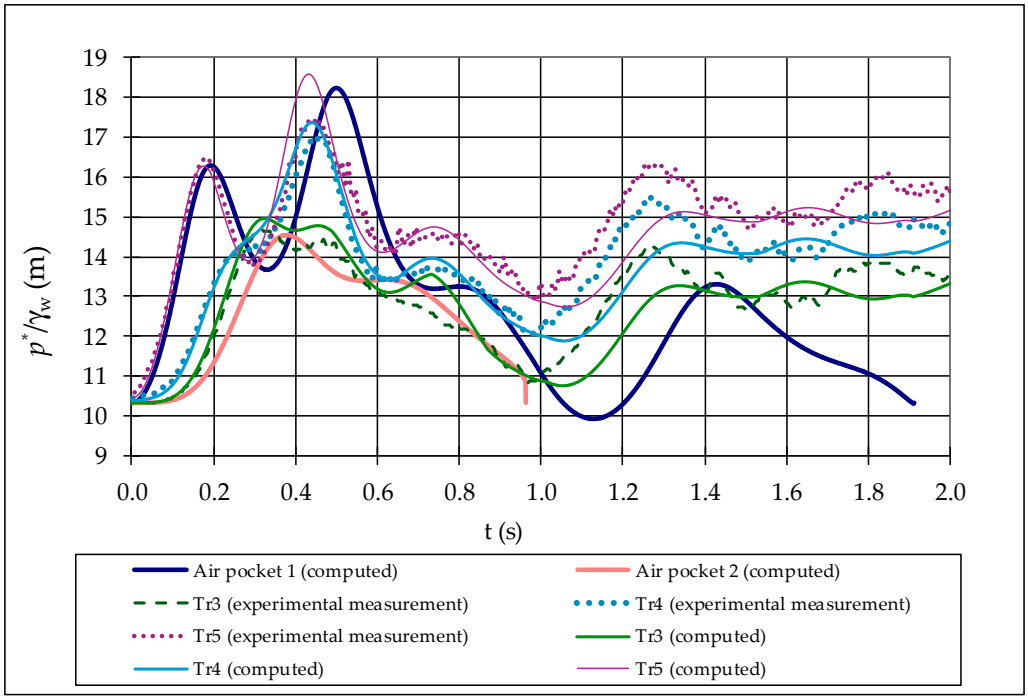

Figure 9. Pressure oscillations during the transient without air valves.

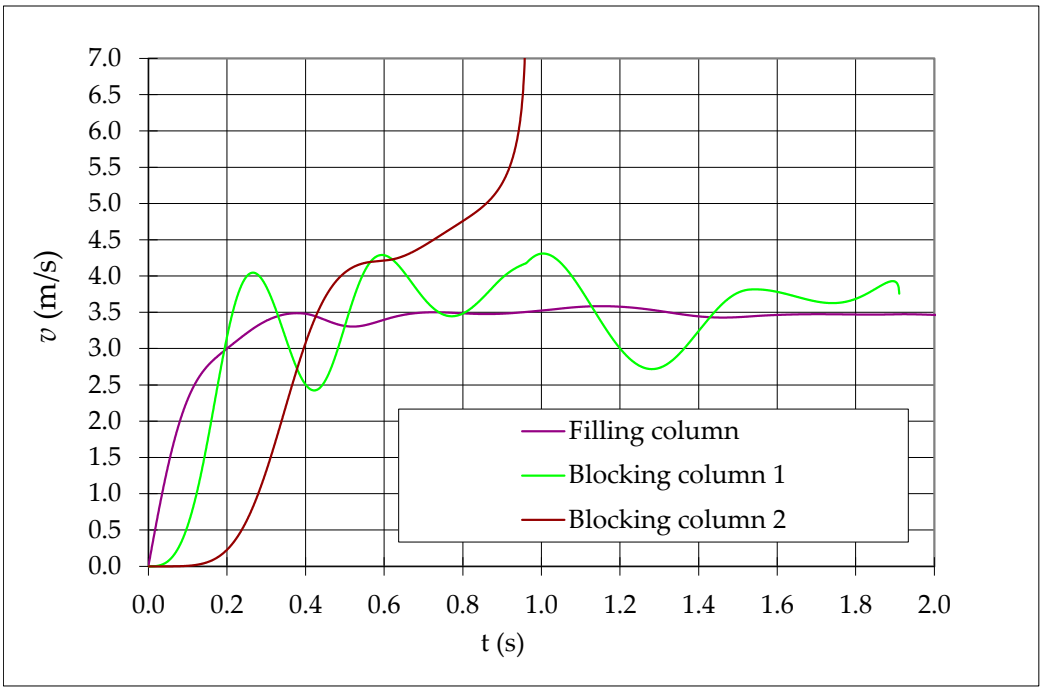

Figure 10. Water velocity pulses during the transient without air valves.

Due to the small size of the studied installation, the transient process lasts only a few seconds. An adiabatic evolution was considered during the experimental stage since entrapped air pockets are rapidly compressed during the transient event, considering that there is no air expulsion. Table 1 presents the times at which the three water columns reach the downstream end of the pipeline.

Table 1. Characteristic times of the transient event without air valves.

Water Column	Time (s)
Blocking column 2 comes out of the installation	0.963
Blocking column 1 comes out of the installation	1.912
The filling column reaches the final point of the installation	2.080

During the initial instant of the transient event, the air pockets compress notably (especially the first one) and reach their maximum pressures. Table 2 presents these maximum values and their corresponding time occurrences.

Table 2. Maximum air pocket pressure heads without air valves.

Type of Peak	Pressure Head (m)	Time (s)
First peak in air pocket 1	$p_1^* = 16.286$	0.193
Second peak in air pocket 1	$p_1^* = 18.230$	0.500
First peak in air pocket 2	$p_2^* = 14.540$	0.379

4.3. Installation Using an Air Valve

This section presents the results considering an air valve located at the highest point of the installation ($x_{V1} = 4.91$ m), which is suitable for expelling air. Table 3 presents the main characteristics of the air valve. An isothermal process was assumed for this analysis, as the air release valves expel air, reducing the likelihood of abrupt changes in the entrapped air pockets.

Table 3. Characteristics of the selected air valve.

Parameter	Value and Units
Expulsion coefficient	$c_{exp} = 0.00028\ (\mathrm{Nm^3/s})/\mathrm{m}$
Cross-sectional area	$A_{exp} = 9.8\ \mathrm{mm^2}$
Internal diameter	$D_{exp} = 3.5$ mm

The air valve has a coefficient $c_{exp} = 0.00028 \frac{\left(\frac{\mathrm{Nm^3}}{\mathrm{s}}\right)}{\mathrm{m}}$, which is suitable of expelling an airflow rate of approximately 8.9 $\frac{\mathrm{Nm^3}}{\mathrm{h}}$ ($Q_{air} = 2.48 \times 10^{-3}\ \frac{\mathrm{Nm^3}}{\mathrm{s}}$) with a differential pressure of 0.5 bar ($\Delta p = 5.1$ m).

The numerical resolution yields the transient evolution shown in Figure 11 (pressure of the two air pockets) and Figure 12 (water velocities of the filling column and the two blocking columns).

It is observed that with the presence of the air vent, the second blocking column comes out of the installation at time $t = 1.259$ s (30% later than filling without the air valve).

The maximum values of air pocket pressure heads considering the installation of an air valve are presented in Table 4.

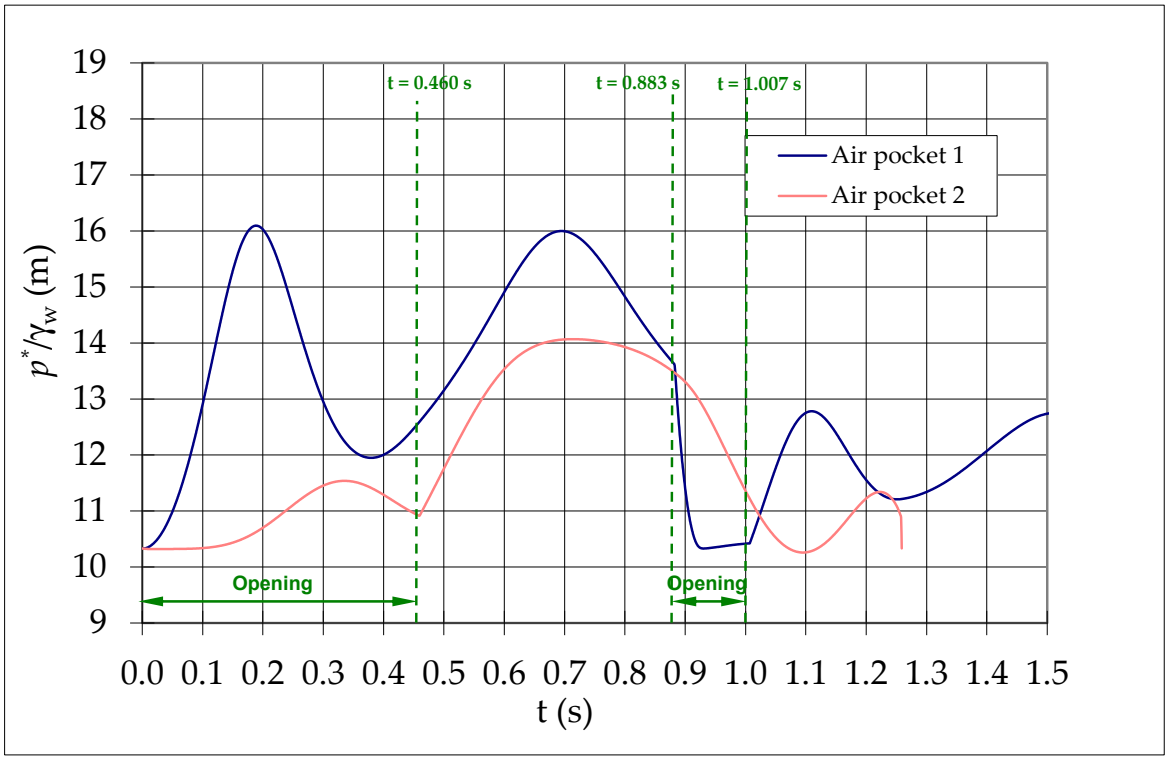

Figure 11. Pressure oscillations during the transient using the air valve.

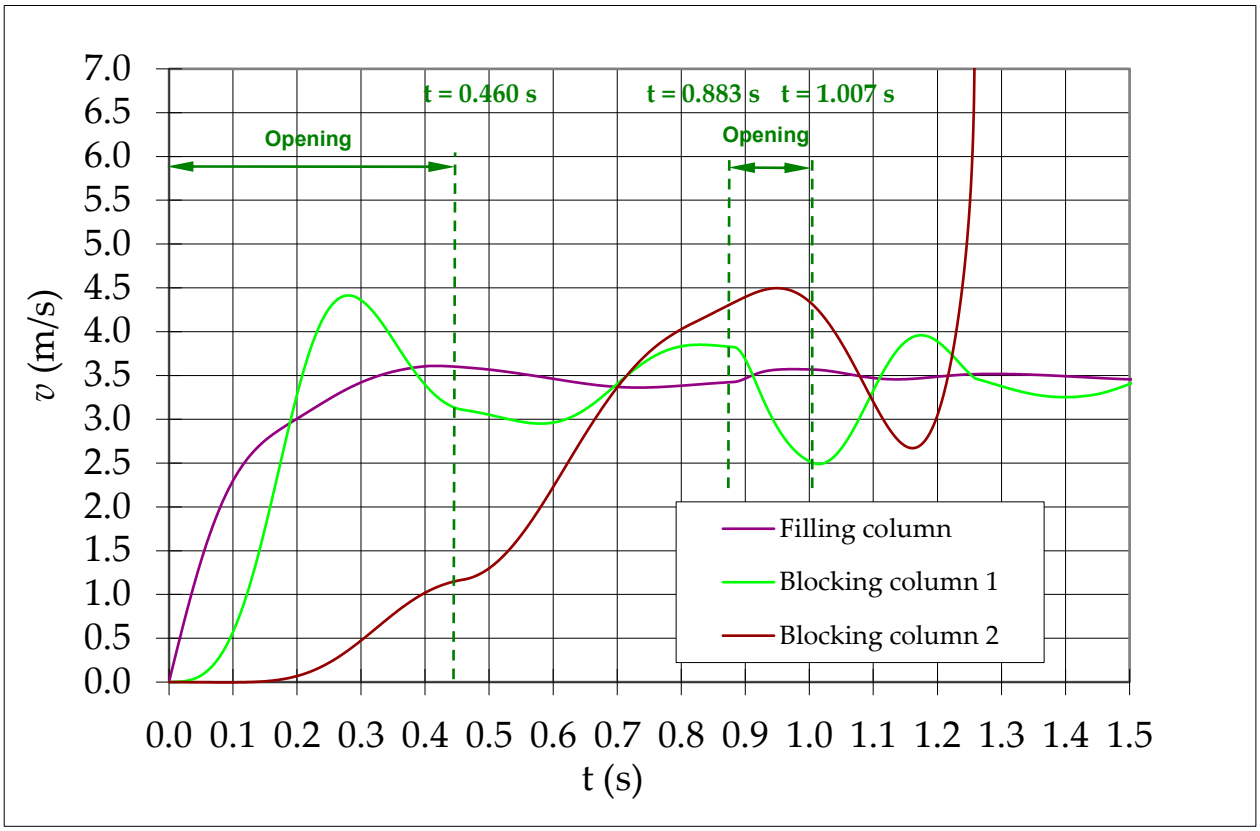

Figure 12. Water velocity pulses during the transient using the air valve.

Table 4. Maximum air pocket pressure heads using the air valve.

Type of Peak	Pressure Head (m)	Time (s)
First peak in air pocket 1	$p_1^* = 16.093$	0.189
Second peak in air pocket 1	$p_1^* = 15.997$	0.695
First peak in air pocket 2	$p_2^* = 11.538$	0.335
Second peak in air pocket 2	$p_2^* = 14.070$	0.714

Initially, the position of the air valve coincides with the second air pocket, so the device is opened and begins expelling air until the corresponding blocking column arrives ($t = 0.460$ s). Throughout this time, the presence of the air valve produces a lower peak of pressure heads compared to when it is neglected. The explanation is straightforward: as the installation fills, the air pocket compresses, causing high-pressure peaks when no air valves are present. The air valve allows the expelling of airflow, preventing the air pocket from compressing as much.

When the water column arrives, the air valve closes and remains closed until another air pocket arrives ($t = 0.883$ s). The air pockets compress, usually with corresponding pressure peaks, since there is no air outlet through the air valve during this period. From the moment the air valve opens again, coinciding with the position of the first air pocket, the pressure in this pocket quickly decreases. The effect of this new opening on the other air pockets is relatively small. The pressure evolution in the first air pocket is smooth until the filling column reaches the pair valve position and closes again ($t = 1.007$ s).

Figure 13 depicts the flow rate and velocity of air expelled through the air valve during the filling procedure. It is observed that during the first opening of the air valve, the maximum expelled flow rate is $Q_{air} = 3.78 \frac{\text{Nm}^3}{\text{h}}$. When the maximum pressure reaches the second air pocket, the maximum flow rate is simultaneously expelled. On the other hand, when the air valve opens for the second time, the pressure in the first air pocket is much higher, consequently increasing the expelled airflow as well ($Q_{air} = 6.66 \frac{\text{Nm}^3}{\text{h}}$ with $v_{air} = 146.7$ m/s).

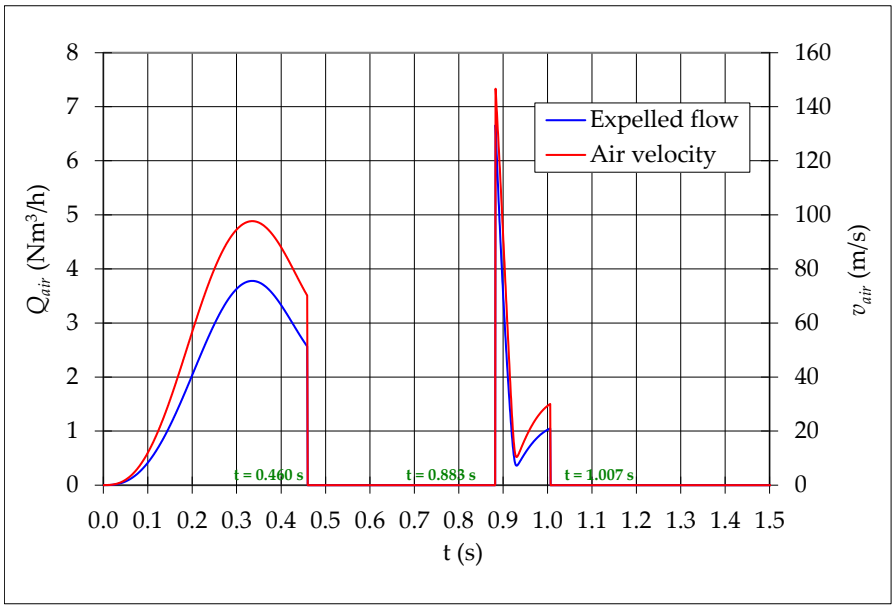

Figure 13. Evolution of expelled air during the transient event.

4.4. Comparison between the Transient Event Considering and Neglecting the Air Valve

After separately analysing the pipeline's filling without air valves and considering them, a comparison was performed, as shown in Figures 14 and 15. Table 5 shows the maximum value of air pocket pressure reached for the two analysed scenarios.

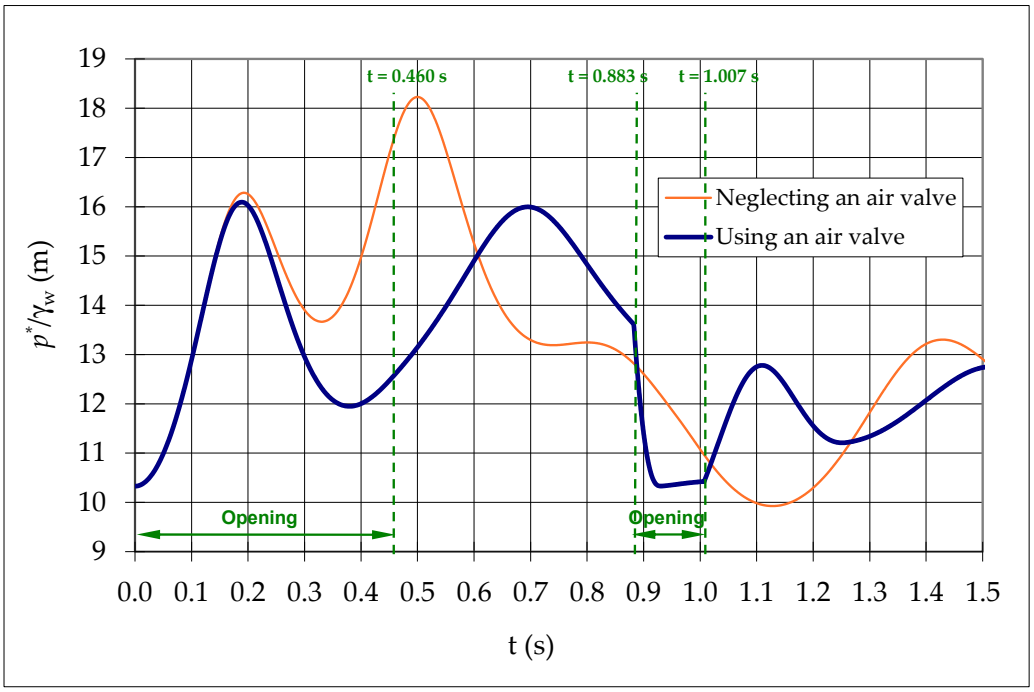

Figure 14. The pressure of the first air pocket p_1^* with and without the air valve.

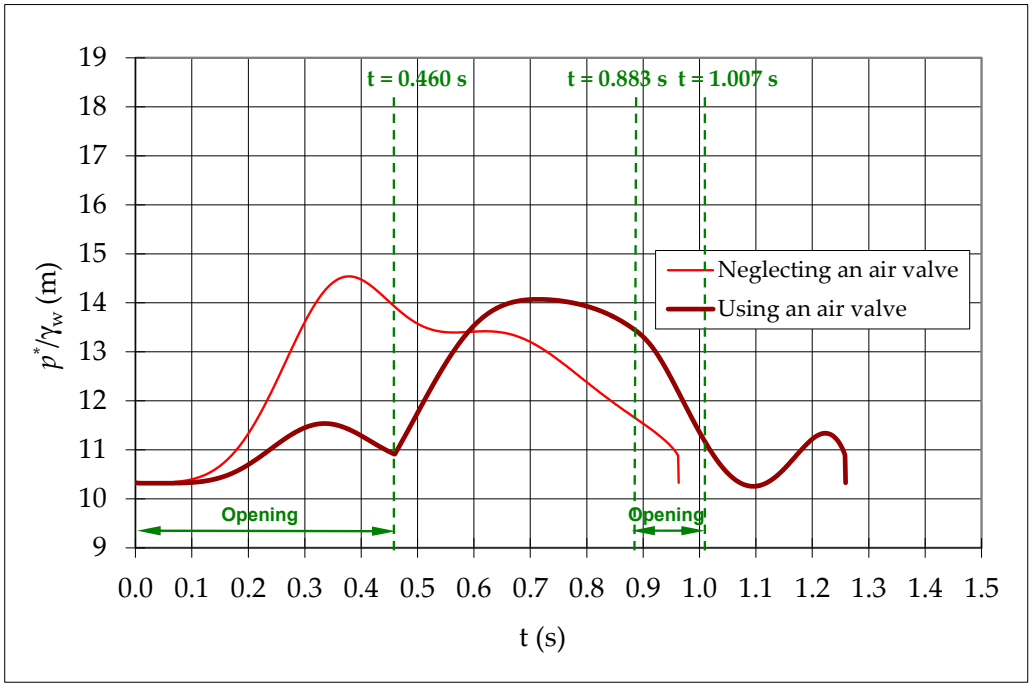

Figure 15. The pressure of the second air pocket p_2^* with and without the air valve.

Table 5. Maximum pressure heads for the first air pocket.

Type of Peak	Without the Air Valve	Considering the Air Valve
First peak in air pocket 1	$p_1^* = 16.286$ m ($t = 0.193$ s)	$p_1^* = 16.093$ m ($t = 0.189$ s)
Second peak in air pocket 1	$p_1^* = 18.230$ m ($t = 0.500$ s)	$p_1^* = 15.997$ m ($t = 0.695$ s)

As expected, the first pressure peak is slightly reduced with the installation of the air valve (16.093 m versus 16.286 m). It should be noted that when the hydraulic installation starts, the filling column abruptly compresses the first air pocket. Still, the first water column reacts much more slowly due to its greater inertia. Therefore, the air valve has almost no effect on the pressure of the first air pocket during these times. Significant differences appear when the first blocking column moves significantly, compressing the second air pocket and causing air to be expelled through the air valve. The second pressure peak is much smaller, with 15.997 and 18.230 m values occurring at 0.695 and 0.500 s, respectively. When the air pocket reaches the air valve position and opens, the pressure drops to nearly atmospheric values. The air pocket begins to compress once more when the air valve closes again as the filling column reaches its position.

Table 6 presents the maximum pressures reached for the second air pocket in the two analysed situations (Figure 15).

Table 6. Maximum pressure heads for the second air pocket.

Type of Peak	Without the Air Valve	Considering the Air Valve
First peak in air pocket 2	$p_2^* = 14.540$ m ($t = 0.379$ s)	$p_2^* = 11.538$ m ($t = 0.335$ s)
Second peak in air pocket 2	$p_2^* = 13.420$ m ($t = 0.620$ s)	$p_2^* = 14.070$ m ($t = 0.714$ s)

The effect of the air valve's installation is evident from the beginning. From the start of the transient event until t = 0.460 s (the period during which the air valve is expelling air), the evolution of the air pocket pressure is much smoother, reaching a maximum value of 11.538 m, which is significantly lower than when the installation fills without the air valve ($p_2^* = 14.540$ m). Once the air valve closes, the air pocket compresses again, generating the corresponding pressure peaks.

Figures 16–18 present the analysis of the evolution of the water velocities for the water columns.

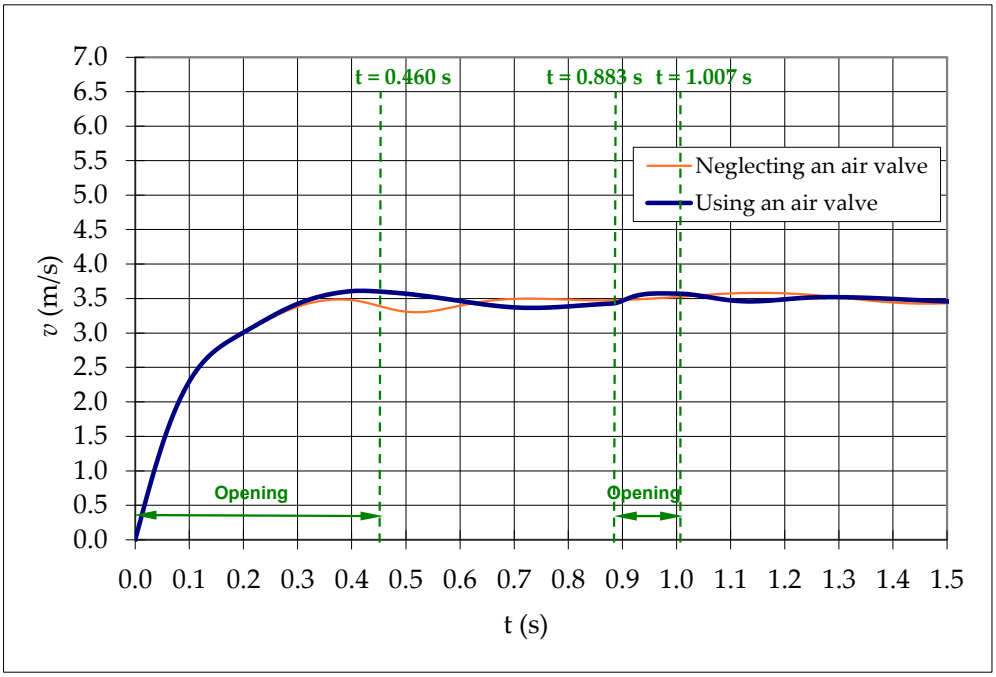

Figure 16. The velocity of the filling column with and without the air valve.

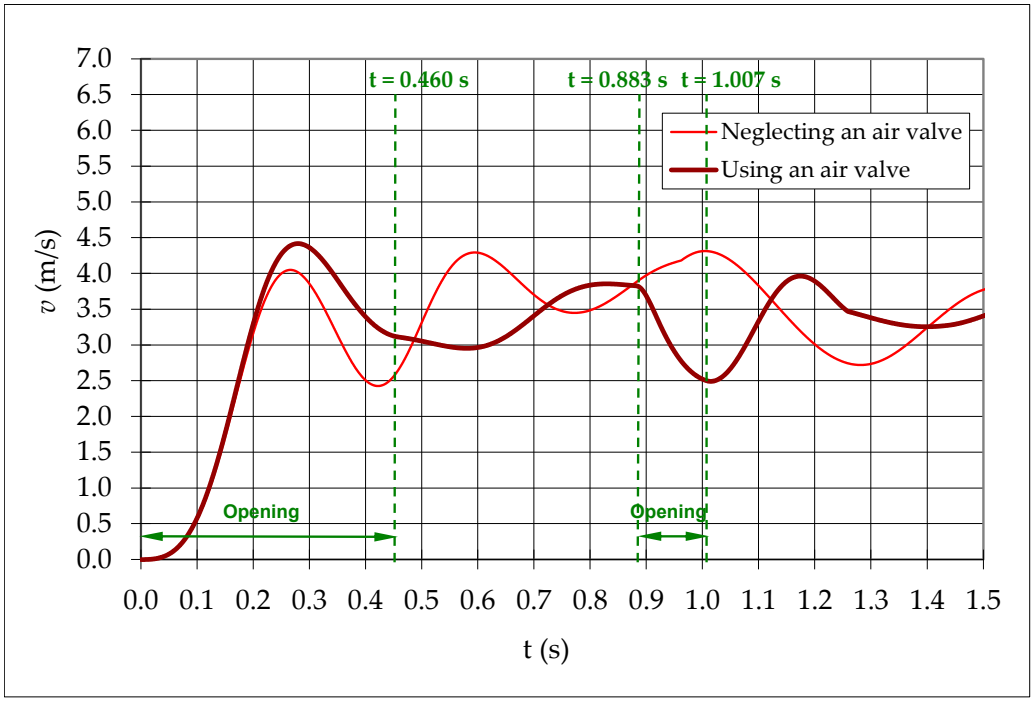

Figure 17. The velocity of the first blocking column v_1 with and without the air valve.

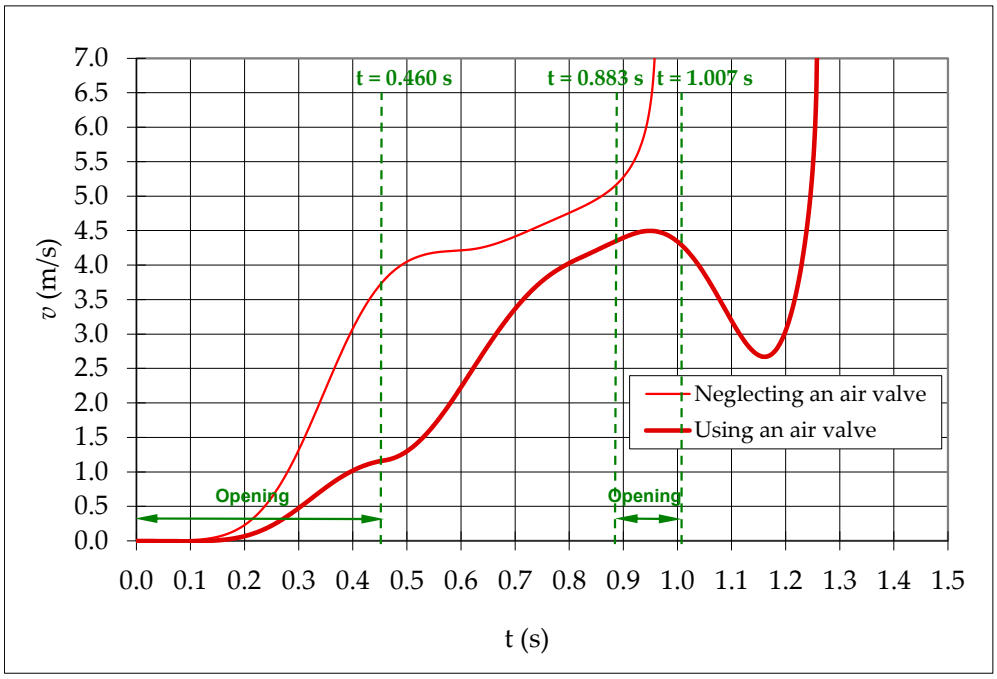

Figure 18. The velocity of the second blocking column v_2 with and without the air valve.

The installation of the air valve affects the velocity of the filling column. The first blocking column's velocity slows down slightly after the beginning of the hydraulic event. However, the movement of the second blocking column is significantly slower when the air valve is installed, as illustrated in Figure 18.

4.5. Comparison of Various Air Valve Sizes

The hydraulic event was analysed, considering the characteristics of the air valve presented in Table 3. The influence of various characteristic curves of air valves is performed.

Table 7 shows three different air valves: the one already studied, a smaller one, and a larger one.

Table 7. Characteristics of the air valves.

Parameter	Air Valve A	Air Valve B	Air Valve C
c_{exp} [(Nm^3/s)/m]	0.00014	0.00028	0.00056
A_{exp} [mm^2]	4.9	9.8	19.6
D_{exp} [mm]	2.5	3.5	5.0

With these expulsion coefficients, for a gauge pressure in the pipe of 0.5 bar, air valve A can expel an airflow rate of $Q_{air} = 4.5\frac{\text{Nm}^3}{\text{h}}$, air valve B can expel an airflow rate of $Q_{air} = 8.9\frac{\text{Nm}^3}{\text{h}}$, and air valve C can expel an airflow rate of $Q_{air} = 17.9\frac{\text{Nm}^3}{\text{h}}$.

Due to their significantly different expulsion capacities, the development of the transient generated will vary notably from one scenario to another. Table 8 shows when each air valve opens and closes during the conduit's filling process.

Table 8. Characteristic times for the different air valves.

Situation	Air Valve A	Air Valve B	Air Valve C
Closure	$t = 0.479$ s	$t = 0.460$ s	$t = 0.445$ s
Opening	$t = 0.886$ s	$t = 0.883$ s	$t = 0.880$ s
Closure	$t = 1.009$ s	$t = 1.007$ s	$t = 1.007$ s

Figure 19 illustrates the pressure evolution of the first air pocket, depicted for the four analysed scenarios: installation without an air valve and considering the three air valves. As observed, during the initial instants of the hydraulic event, the influence of the air valve is practically negligible. When the air valve closes, a compression process of the air pocket begins, which varies for each scenario depending on the specific conditions of the closure's occurrence. For instance, with the most oversized air valve, a higher second peak pressure is reached (p_2^* = 18.280 m), slightly exceeding the pressure obtained without air valves.

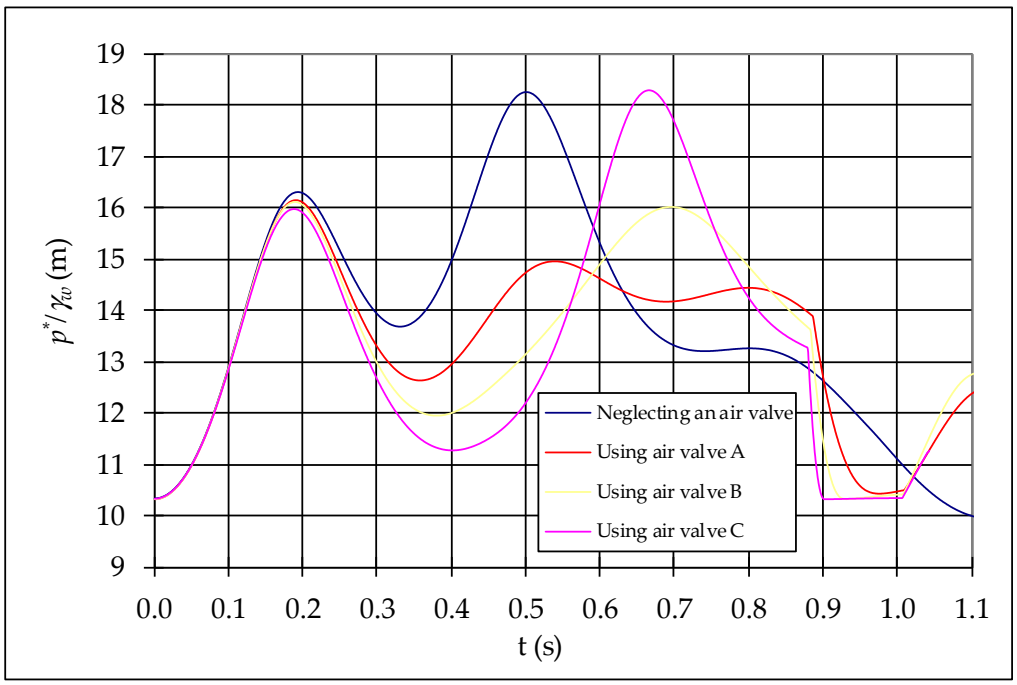

Figure 19. The pressure pulses of the first air pocket p_1^* for different air valves.

Figure 20 presents the effect of the air valve size on the transient occurring during the filling manoeuvre. It shows the pressure evolution of the second air pocket. Table 9 shows the value of the first pressure peak, the time when the maximum pressure is reached, and the time for the first closure of the air valve.

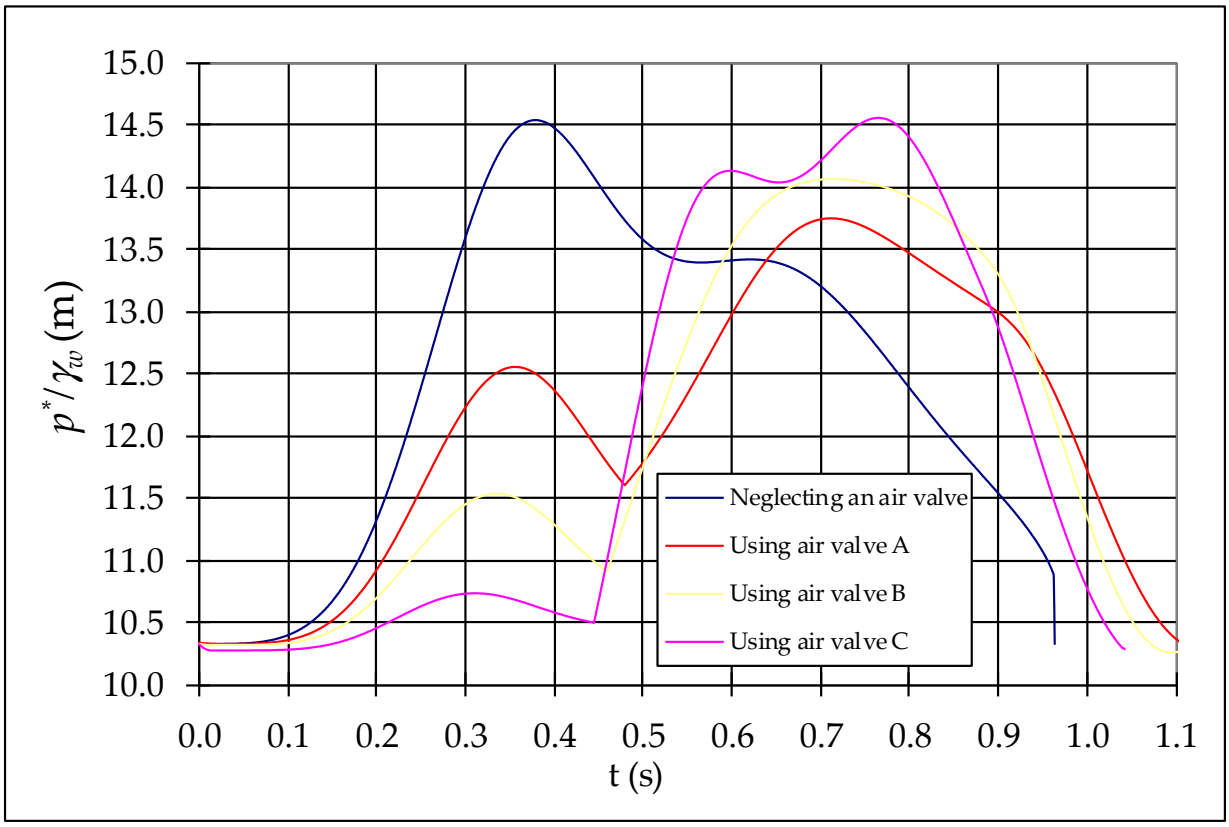

Figure 20. The pressure pulses of the second air pocket p_2^* for different air valves.

Table 9. Results for the different air valves (second air pocket).

Variable		Air Valve A	Air Valve B	Air Valve C
Maximum air pocket pressure	Value (m)	12.551	11.538	10.739
	Time (s)	0.356	0.335	0.311
Time closure (s)		0.479	0.460	0.445

Table 9 shows the influence of the air valve size on the hydraulic event. The greater the air valve's expulsion capacity, the lower the pressure peak. This peak is reached earlier and the air valve closes sooner due to the arrival of the water column.

When the air valve closure is produced, the air pockets compress, reaching their corresponding pressure peaks. Considering the air valve closure, the highest-pressure peak in the hydraulic installation occurs using the most oversized air valve (see Figure 20); since the air valve is not active, the air cannot be expelled, reducing the pressure peaks. Figure 21 illustrates the expelled flow rate of the three air valves during the transient event, while Figure 22 shows the air velocity through the outlet orifice.

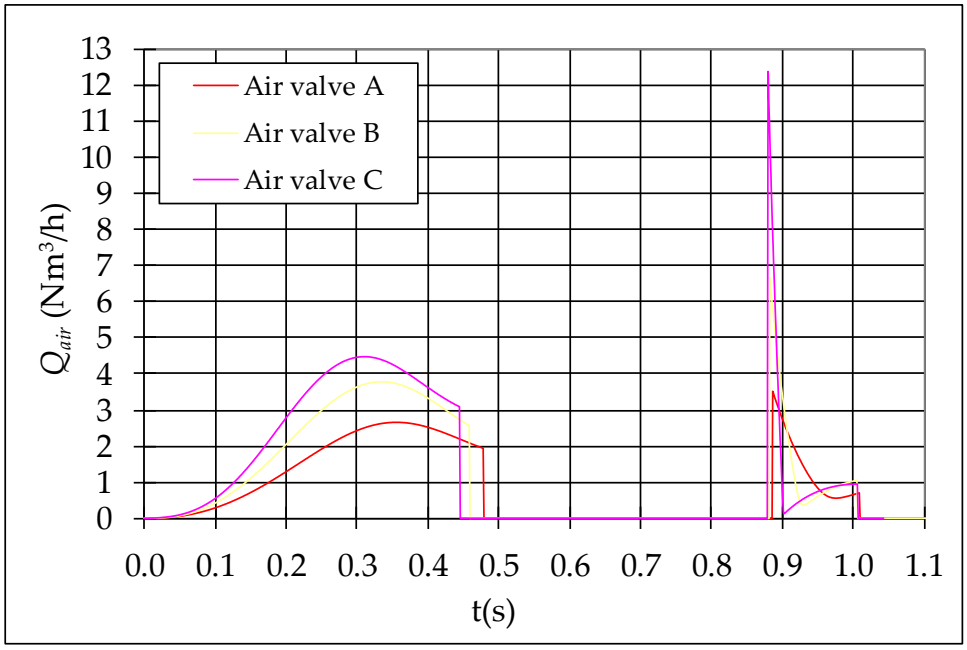

Figure 21. Expelled airflow rate Q_{air} through the different air valves.

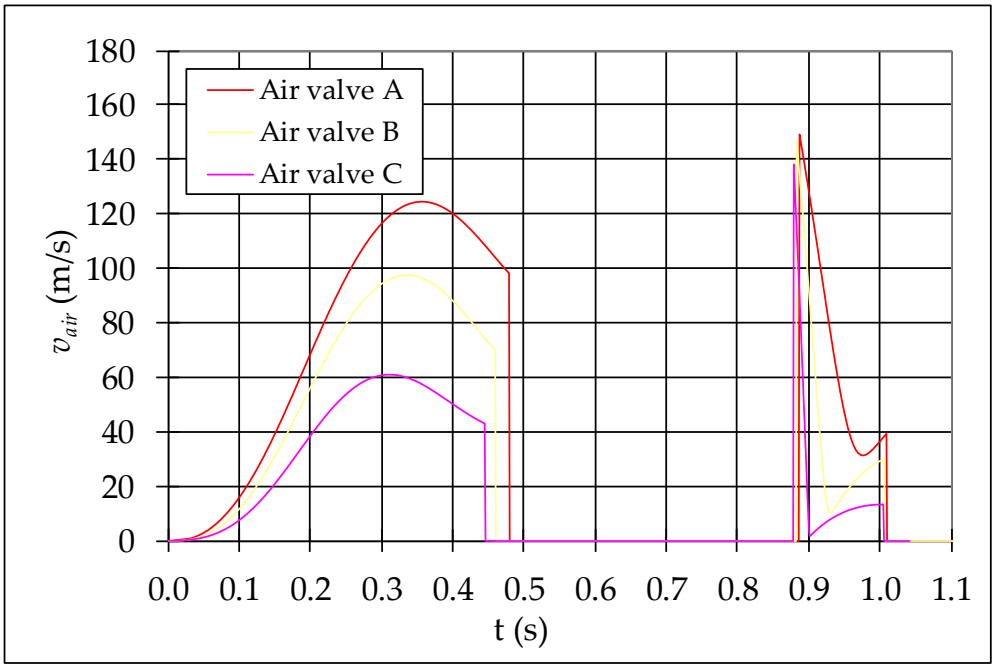

Figure 22. Air velocity v_{air} through the different air valves.

5. Conclusions

A general mathematical model based on the Rigid Column Model has been developed to analyse transient events generated by n entrapped with air pockets in water pipelines with irregular profiles, incorporating various air valves. The proposed model's main advantage over the previous models is that it considers the effect of blocking columns, even considering the impact of expelled air. The findings from the analysed small experimental facility cannot be directly extrapolated to actual pipelines.

Based on this research, it is crucial to consider the following:

- Model Applicability: The model proposed in this research can serve as a starting point for water utilities to compute the maximum pressure of entrapped air pockets during filling operations in water installations.
- Avoiding Blocking Columns: Blocking columns should be avoided in actual pipelines as they can generate hazardous pressure surges by compressing trapped air pockets. Water utilities must ensure that pipelines are wholly drained before filling operations commence. The placement of draining valves should guarantee complete drainage before starting up the pipelines.
- Controlled Filling: Pipeline filling should be conducted slowly to facilitate the expulsion of air through the valves. Care must be taken when filling pipelines with trapped air, as even with air valves installed, complete system safety cannot be guaranteed.
- Air Valve Selection: It is advisable to choose a reliable air valve manufacturer for sizing water installations to ensure proper characterisation of the differential pressure-versus-airflow curve.
- Polytropic Evolution: Selecting the appropriate polytropic process remains challenging for engineers and designers, as determining a specific value for real-world water installations is complex. This research recommends that an adiabatic behaviour should be considered for rapid transient flows, while an isothermal behaviour is more appropriate for slower events. Intermediate values may be adopted depending on the scenarios under consideration.
- Numerical Resolution: The filling procedure involves solving a system of differential-algebraic equations, which was addressed using an adaptive fifth-order Runge-Kutta method.

Author Contributions: Conceptualization, V.S.F.-M., A.A.-P. and O.E.C.-H.; methodology, A.A.-P. and O.E.C.-H.; formal analysis, O.E.C.-H.; validation, A.A.-P. and V.S.F.-M.; writing—original draft preparation, A.A.-P. and O.E.C.-H.; writing—review and editing, V.S.F.-M. All authors have read and agreed to the published version of the manuscript.

Funding: This research received no external funding.

Data Availability Statement: Databases are available in this article.

Conflicts of Interest: The authors declare no conflicts of interest.

References

1. Pozos-Estrada, O.; Pothof, I.; Fuentes-Mariles, O.A.; Dominguez-Mora, R.; Pedrozo-Acuña, A.; Meli, R.; Peña, F. Failure of a Drainage Tunnel Caused by an Entrapped Air Pocket. *Urban Water J.* **2015**, *12*, 446–454. [CrossRef]
2. Wang, L.; Wang, F.; Karney, B.; Malekpour, A. Numerical Investigation of Rapid Filling in Bypass Pipelines. *J. Hydraul. Res.* **2017**, *55*, 647–656. [CrossRef]
3. Ferreira, J.P.; Ferràs, D.; Covas, D.I.C.; van der Werf, J.A.; Kapelan, Z. Air Entrapment Modelling during Pipe Filling Based on SWMM. *J. Hydraul. Res.* **2024**, *62*, 39–57. [CrossRef]
4. Fuertes-Miquel, V.S.; Coronado-Hernández, O.E.; Mora-Meliá, D.; Iglesias-Rey, P.L. Hydraulic Modeling during Filling and Emptying Processes in Pressurized Pipelines: A Literature Review. *Urban Water J.* **2019**, *16*, 299–311. [CrossRef]
5. Ferreira, J.P.; Ferràs, D.; Covas, D.I.C.; Kapelan, Z. Air Entrapment Modelling in Water Supply Networks during Pipe Filling Events. *Urban Water J.* **2024**, *21*, 685–697. [CrossRef]
6. Tasca, E.S.A.; Karney, B. Improved Air Valve Selection through Better Device Characterization and Modeling. *J. Hydraul. Eng.* **2023**, *149*, 4023019. [CrossRef]
7. Apollonio, C.; Balacco, G.; Fontana, N.; Giugni, M.; Marini, G.; Piccinni, A.F. Hydraulic Transients Caused by Air Expulsion During Rapid Filling of Undulating Pipelines. *Water* **2016**, *8*, 25. [CrossRef]
8. Fontana, N.; Galdiero, E.; Giugni, M. Pressure Surges Caused by Air Release in Water Pipelines. *J. Hydraul. Res.* **2016**, *54*, 461–472. [CrossRef]
9. American Water Works Association (AWWA). *Air-Release, Air/Vacuum, and Combination Air Valves: M51*; American Water Works Association: Denver, CO, USA, 2001.
10. Tran, P.D. Pressure Transients Caused by Air-Valve Closure While Filling Pipelines. *J. Hydraul. Eng.* **2017**, *143*, 4016082. [CrossRef]
11. Pozos, O.; Gonzalez, C.A.; Giesecke, J.; Marx, W.; Rodal, E.A. Air Entrapped in Gravity Pipeline Systems. *J. Hydraul. Res.* **2010**, *48*, 338–347. [CrossRef]

12. Zhou, L.; Cao, Y.; Karney, B.; Bergant, A.; Tijsseling, A.S.; Liu, D.; Wang, P. Expulsion of Entrapped Air in a Rapidly Filling Horizontal Pipe. *J. Hydraul. Eng.* **2020**, *146*, 4020047. [CrossRef]
13. Huang, B.; Fan, M.; Liu, J.; Zhu, D.Z. CFD Simulation of Air–Water Interactions in Rapidly Filling Horizontal Pipe with Entrapped Air. In Proceedings of the World Environmental and Water Resources Congress, Online, 7–11 June 2021; pp. 495–507. [CrossRef]
14. Iglesias-Rey, P.L.; Fuertes-Miquel, V.S.; García-Mares, F.J.; Martínez-Solano, J.J. Comparative Study of Intake and Exhaust Air Flows of Different Commercial Air Valves. *Procedia Eng.* **2014**, *89*, 1412–1419. [CrossRef]
15. Martin, C.S. Entrapped Air in Pipelines. In Proceedings of the 2nd International Conference on Pressure Surges, British Hydromechanics Research Assoc., London, UK, 22–24 September 1976; pp. 5–28.
16. Liou, C.P.; Hunt, W.A. Filling of Pipelines with Undulating Elevation Profiles. *J. Hydraul. Eng.* **1996**, *122*, 534–539. [CrossRef]
17. Izquierdo, J.; Fuertes, V.S.; Cabrera, E.; Iglesias, P.L.; Garcia-Serra, J. Pipeline Start-up with Entrapped Air. *J. Hydraul. Res.* **1999**, *37*, 579–590. [CrossRef]
18. Wylie, E.B.; Streeter, V.L. *Fluid Transients*; Advanced Book Program; McGraw-Hill International Book Company: New York, NY, USA, 1978.
19. Zhou, L.; Liu, D.; Karney, B. Investigation of Hydraulic Transients of Two Entrapped Air Pockets in a Water Pipeline. *J. Hydraul. Eng.* **2013**, *139*, 949–959. [CrossRef]
20. Fuertes-Miquel, V.S. Hydraulic Transients with Entrapped Air Pockets. Ph.D. Thesis, Polytechnic University of Valencia, Valencia, Spain, 2001.
21. Tijsseling, A.S.; Hou, Q.; Bozkuş, Z.; Laanearu, J. Improved One-Dimensional Models for Rapid Emptying and Filling of Pipelines. *J. Press. Vessel Technol.* **2015**, *138*, 031301. [CrossRef]
22. Zhou, L.; Liu, D.; Karney, B.; Wang, P. Phenomenon of White Mist in Pipelines Rapidly Filling with Water with Entrapped Air Pockets. *J. Hydraul. Eng.* **2013**, *139*, 1041–1051. [CrossRef]
23. Zhou, L.; Liu, D.; Karney, B.; Zhang, Q. Influence of Entrapped Air Pockets on Hydraulic Transients in Water Pipelines. *J. Hydraul. Eng.* **2011**, *137*, 1686–1692. [CrossRef]